FERMILAB-PUB-11-420-AD

Preprint typeset in JINST style - HYPER VERSION

The Tevatron Wide Band Longitudinal Coupled Bunch Mode Dampers – an account from Its commissioning to its decommissioning

Cheng-Yang Tan[a] **and James Steimel**[a]

[a] *Fermi National Accelerator Laboratory,*
P.O. Box 500, Batavia, IL 60510-5011
E-mail: cytan@fnal.gov

ABSTRACT: The Tevatron longitudinal dampers were built in 2002 to stop the proton beam from spontaneously blowing up during high energy physics. The system has been operational since then and has been very successful in keeping the beam stable. In October 2011, the Tevatron will be shutdown and the dampers decommissioned. The goal of this paper is to document the 9 year experience in the operation of these dampers, account for the design choices made at the time, describe its commissioning, and its performance during its working life. Included will be a discussion on the type of instability which required the damper to be built.

KEYWORDS: Hardware and accelerator control systems..

Contents

1. Introduction **1**
- 1.1 Effects on luminosity and background losses 3
- 1.2 Coupled Bunch Mode Instability 3

2. Theory **4**

3. Hardware Setup **7**
- 3.1 Equalizer 8
- 3.2 Phase Shifter 9
- 3.3 Notch Filter 10
  - 3.3.1 Differentiator 10
- 3.4 Near Uniform Triggers 11
- 3.5 Phase Shifts 12
- 3.6 Problem with Mode 0 12
- 3.7 Setting up the 1 turn delay 13
- 3.8 Making the notches 14
- 3.9 Limits on the gain 14
- 3.10 Tests 14

4. Damper Performance during Stores **14**

5. Conclusion **15**

A. Some Parameters of the Tevatron **15**

1. Introduction

When Run II began in its first year, the high current stored in the Tevatron caused unforeseen problems in the beam dynamics. These needed to be fixed before higher luminosities could be achieved. One of the problems that started to appear at the beginning of 2002 was the rapid blow up of the longitudinal beam size during a store. See Figure 1. Although these blow ups do not appear in every store, they seem to be weakly correlated with beam current. At that time, there were conjectures that coupled bunch mode instabilities that arose from coupling to the higher order parasitic modes of the RF cavities are the cause of the instabilities. As the frequency of these higher modes move as a function of temperature, the coupled bunch modes can be stable or unstable depending on where and how the higher order parasitic modes line up. Table 1 shows eleven stores in the month of May 2002 where about $2/3$ of the stores were unstable. Note: The "before blow up" time is measured w.r.t. the time flattop is reached.

Table 1. Comparison of different stores

Store	Date	Num. protons $\times 10^{11}$	Bunch length before blow up (ns)	Bunch length after blow up (ns)	Time before blow up (min)	$1/e$ time before blow up (hr)	$1/e$ time after blow up (hr)	Comments
1302	8 May 02	1.70	2.0	2.3	60	42	67	
1305	9 May 02	1.67	2.0	2.3	6	12	43	
1307	10 May 02	1.79	2.0	–	–	53	–	No blow up
1309	11 May 02	1.71	2.0	–	–	42	–	No blow up
1313	12 May 02	1.76	2.0	–	–	40	–	No blow up
1329	16 May 02	1.76	1.9	2.2	3	No data	77	
1332	17 May 02	1.78	1.9	2.4	6	9	83	
1333	18 May 02	1.81	2.1	–	–	50	–	No blow up
1335	19 May 02	1.77	2.0	2.2	39	40	59	
1337	20 May 02	1.83	2.0	2.2	16	19	56	
1340	21 May 02	1.94	2.0	2.6	2	No data	No data	

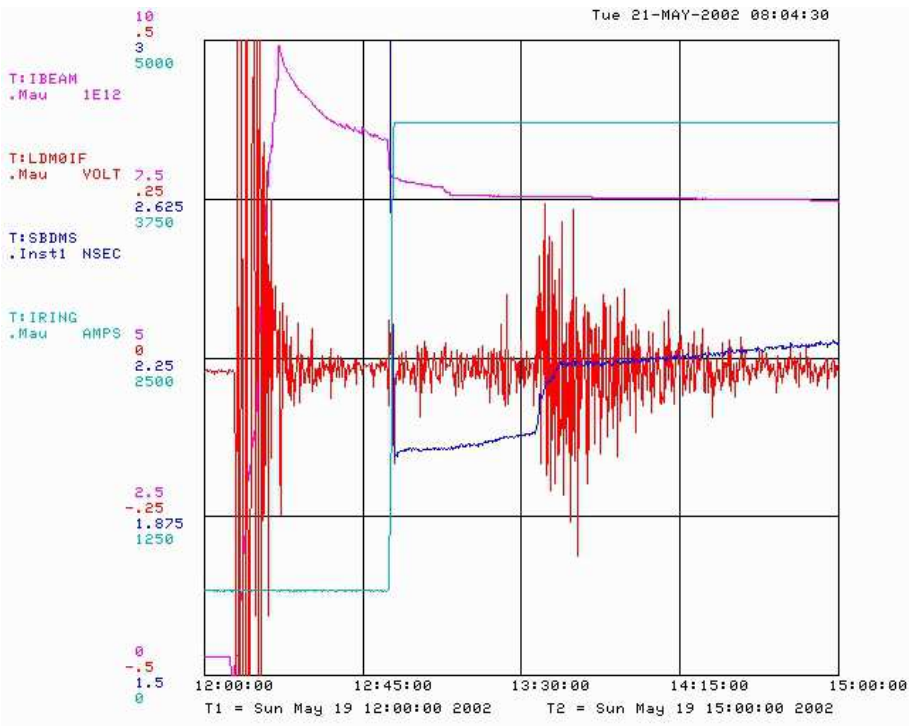

Figure 1. The beam blows up longitudinally (rms bunch length – T:SBDMS) at about 1340hrs during the store which started at about 1300hrs. We see that when it blows up the phase of the bunch oscillates w.r.t. the RF (amplitude of the oscillation– T:LDM0IF). Plotted also are beam current T:IBEAM and the magnet bus current T:IRING.

The instability could not be controlled with narrow band (mode 0) dampers. This showed us that the instability may be a longitudinal head-tail or higher order coupled bunch mode. At the time,

we did not have the instrumentation to distinguish between the two types, but later experiments showed that the longitudinal instability was indeed mode 1 coupled bunch mode instability. See section 1.2.

The attitude in 2002 was to stop the beam from blowing up at all cost and to do it very quickly because this instability not only caused unacceptable beam loss at the experiments, it also caused a drop in luminosity. See section 1.1. The problem for us was that the type of instability was an unknown and so building a narrow band damper system was too much of a risk.

We decided to build a wide band longitudinal damper system that would take care of all the coupled bunch mode instabilities (except mode 0) because of the strong time pressures for solving this problem.[1] In our design, we used the accelerating cavities as its kicker which meant that we had to take into account their high Q (10^4) and the rapidity of their impedance fall off away from resonance. Furthermore, the amplitude and phase response is not constant for all synchrotron sideband pairs, and thus the response of the dampers for the mode 1 coupled bunch mode would be an order of magnitude greater than the higher order coupled bunch modes. It would have been impossible to keep the feedback stable for mode 1 and still have useful gain at the higher order modes. We overcame this problem by building an equalizer that leveled the impedance so that it looked constant away from the resonance. Besides the equalizer, the damper also needed a notch filter that suppressed the revolution harmonics (otherwise these harmonics would limit the gain of the loop) and differentiated in time the synchrotron sidebands. Lastly, we also had to time in the system so that the error signal of bunch n was applied exactly one turn later to kick bunch n.

1.1 Effects on luminosity and background losses

When the bunch length suddenly grows, the luminosity at the experiments drops quickly and also causes long persistent background losses at the experiments.

The effect on luminosity is shown in Figure 2. The increase in bunch length by 8.8% causes a drop of $\sim$2% of at CDF and 1.6% at D0. Note: The CDF data shown here is much noisier than D0 and despite an initial luminosity drop from the bunch length growth, it increases again when the bunch length is shaved away in the high dispersion areas of the Tevatron. Interestingly, D0 does not see an increase when the bunch length decreased.

The effect on background losses at the CDF experiment are shown in Figure 3 which increases by at a factor of 4 when the bunch length suddenly grows. It is only when the collimators are withdrawn and the beam no longer scrapes on them that the losses get under control.

1.2 Coupled Bunch Mode Instability

It is not until much later that the type of instability was identified to be coupled bunch mode 1 when better instrumentation and software became available. The Tevatron SBD (sampled bunch display [1]) was used to collect the centroid data of each bunch shown in Figure 4. Each frame shows the position of the 36 bunch centroids w.r.t. its position *before* the onset of the instability in consecutive frames which are taken 2 s apart. Frame 1 shows the onset of the instability where

[1] Clearly, there are other ways to stop the instabilities *if* we were confident as to the source, e.g. lowering the impedance of the RF cavities [2, 3]. However, although the RF cavities are the most likely candidates for the source of the instability, there are other large impedance devices in the Tevatron, e.g. Lambertsons.

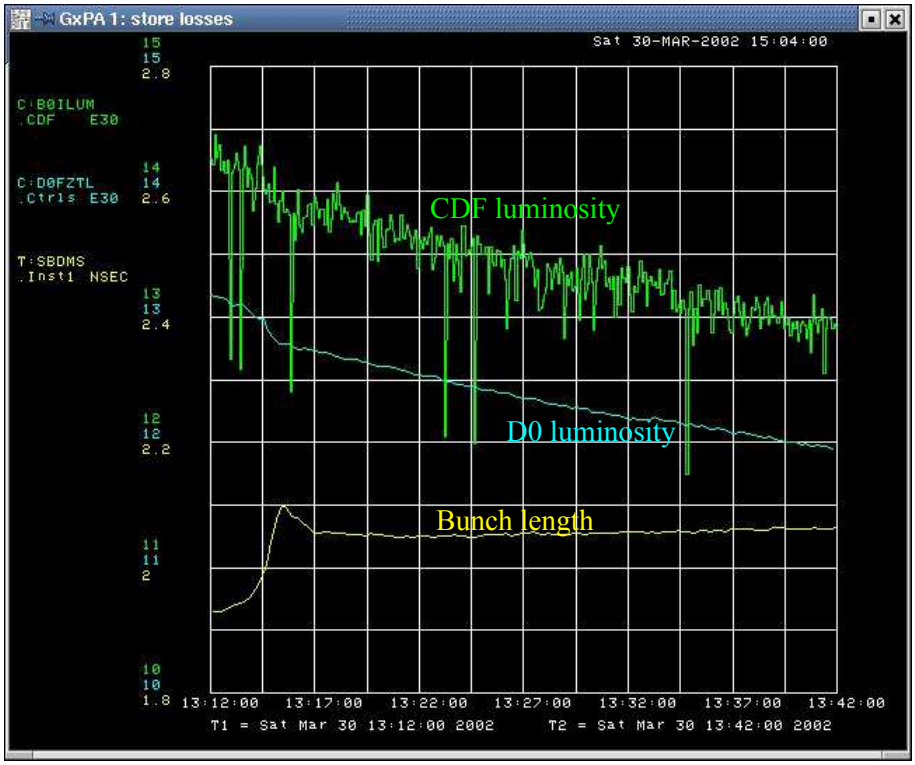

Figure 2. The luminosity at the experiments CDF (C:B0ILUM) and D0 (C:D0FZTL) and the median rms bunch length (T:SBDMS) are plotted here. The bunch length growth from the instability drops the luminosity at both experiments.

the mode 1 pattern just begins. This pattern becomes very clear in frames 4, 5 and 6 where the centroids can have a maximum amplitude of 49°. This pattern starts to dissipate after frame 7.

The source of the instability is still not completely understood even after 9 years of operations. The most likely impedance candidates are the RF cavity fundamental mode or a parasitic mode at 311 MHz.

2. Theory

Let us consider a simple damper system shown in Figure 5. The source of this derivation comes from D. McGinnis [4]. Looking at Figure 5, Z_E represents the impedance of the electronics and G_B represents the conductance of the beam. Therefore,

$$I_G = G_B V_{\text{out}} \tag{2.1}$$

and the output voltage V_{out} of the damper is

$$\begin{aligned} V_{\text{out}} &= Z_E \left(I_{\text{in}} + I_G \right) \\ &= Z_E \left(I_{\text{in}} + G_B V_{\text{out}} \right) \end{aligned} \tag{2.2}$$

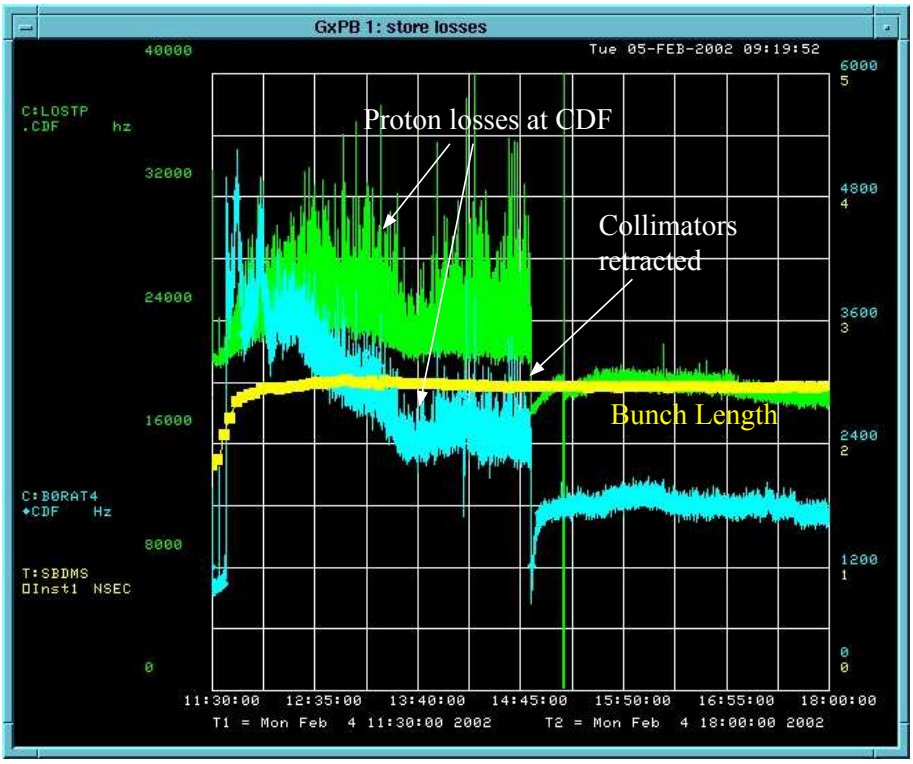

Figure 3. The sudden bunch length growth (T:SBDMS) causes the losses at CDF to increase and become very spiky (C:LOSTP and C:B0RAT4). The sudden drop in losses comes from the withdrawal of collimators.

Solving for the impedance of the entire system Z_D, we have

$$Z_D(s) = \frac{V_{\text{out}}}{I_{\text{in}}} = \frac{Z_E(s)}{1 - G_B(s)Z_E(s)} \tag{2.3}$$

So, if we examine Eq. 2.3, we can see in its denominator is $G_B Z_E$, which is the open loop response of the damper system. To determine the stability of the damper system, let Z_E be of finite bandwidth with one pole, i.e.

$$Z_E \equiv \frac{Z'_E}{1 + \alpha s} \tag{2.4}$$

Then

$$Z_D = \frac{Z'_E}{\alpha\left(s + \frac{1 - G_B Z'_E}{\alpha}\right)} \tag{2.5}$$

which implies that the pole is at

$$s_p = -\frac{1 - G_B Z'_E}{\alpha} \tag{2.6}$$

and thus by inverse Laplace transforming Eq. 2.5, we have the temporal response W_D of the damper

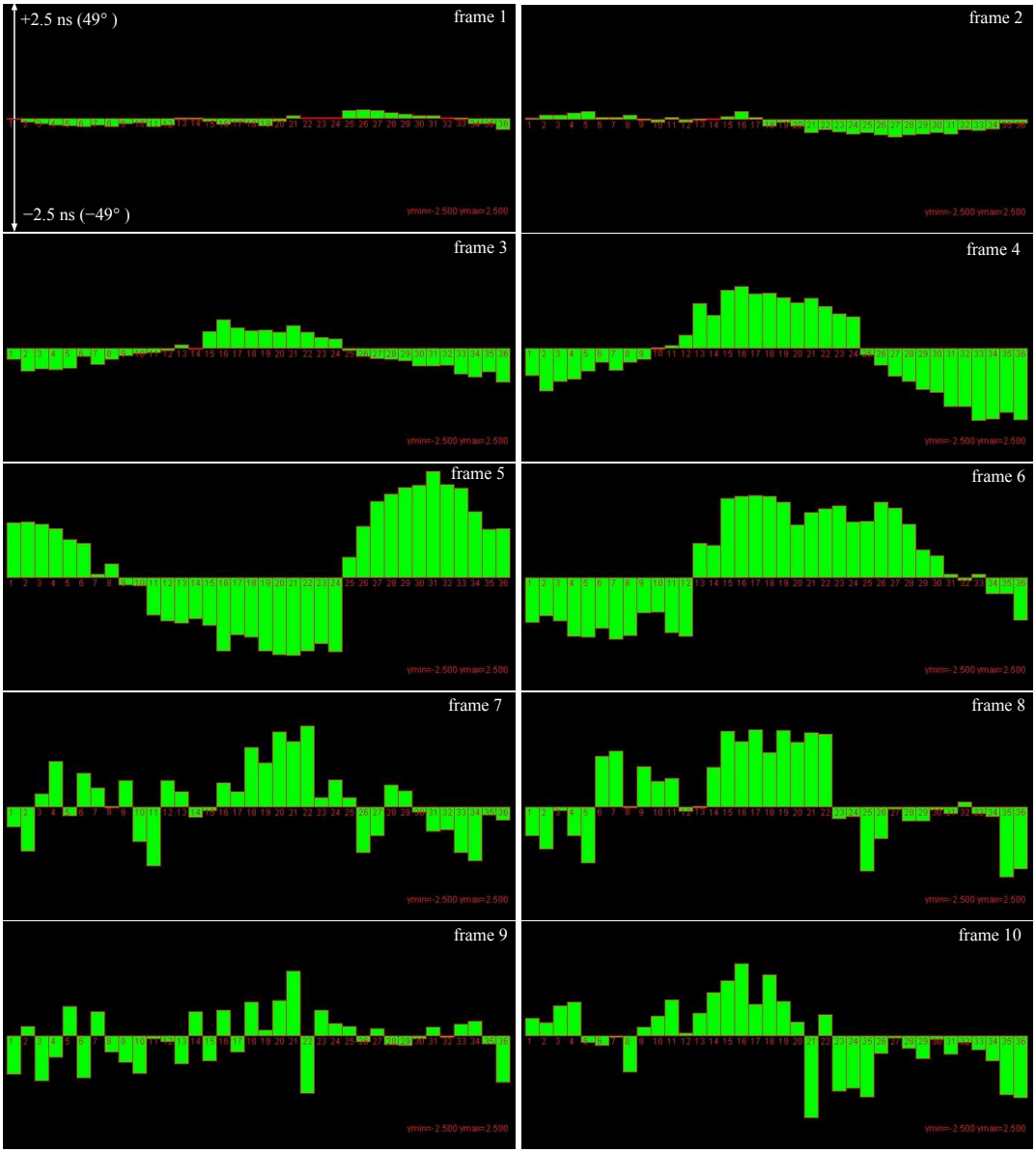

Figure 4. These frames, which are taken 2 s apart, show the time evolution of the instability for the 36 bunches in the Tevatron for store 3918 (11 Jan 2005) where the longitudinal dampers were accidentally disabled. Each green box is the centroid position of the bunch w.r.t. its position *before* the instability. Frames 3, 4, 5 and 6 clearly show a mode 1 coupled bunch mode pattern.

system

$$
\begin{aligned}
W_D(t) &\sim e^{s_p t} \\
&= e^{-\frac{1-\mathrm{Re}\left[G_B Z'_E\right]}{\alpha} t} \times e^{i\mathrm{Im}\left[G_B Z'_E\right] t} \\
&= (\text{decay or growth part}) \times (\text{oscillatory part})
\end{aligned}
\tag{2.7}
$$

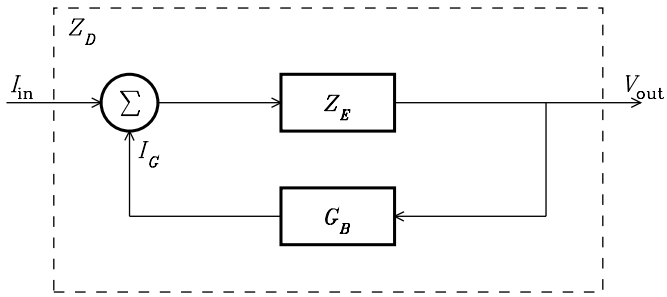

Figure 5. This is a block diagram of a simple damper system.

Clearly, for dampers we want the decay part of Eq. 2.7, thus

$$1 - \text{Re}\left[G_B Z_E'\right] > 0 \tag{2.8}$$

or

$$\text{Re}\left[G_B Z_E'\right] < 1 \tag{2.9}$$

which means that the real part of the open loop response must be < 1 for damping. This is the most important result of this section.

3. Hardware Setup

In this section, we will go through each part of our setup used for our bunch by bunch longitudinal dampers and show that the open loop response $G_B Z_E' < 1$. Figure 6 is a block diagram of the setup. The damper system starts at the stripline pickups which sum the beam signals at the two plates to produce a signal which is proportional to the longitudinal position of the beam. This signal is then down converted with the Tevatron RF (53 MHz) to produce a phase error (or quadrature) signal w.r.t. it. The error signal is then processed with electronics which perform the following:

(i) Equalize the impedance of the RF cavity.

(ii) Suppress the revolution harmonics and differentiate the synchrotron sidebands around the revolution lines.

(iii) One turn delay so that when the dampers pick up the signal of bunch 1 it will kick bunch 1 one turn later.

To accomplish (i), we have a high pass filter (hpf) which equalizes the RF cavity impedance and for (ii), we have notch filters at every revolution harmonic. For (iii) we have a digital delay and a near uniform triggering system.

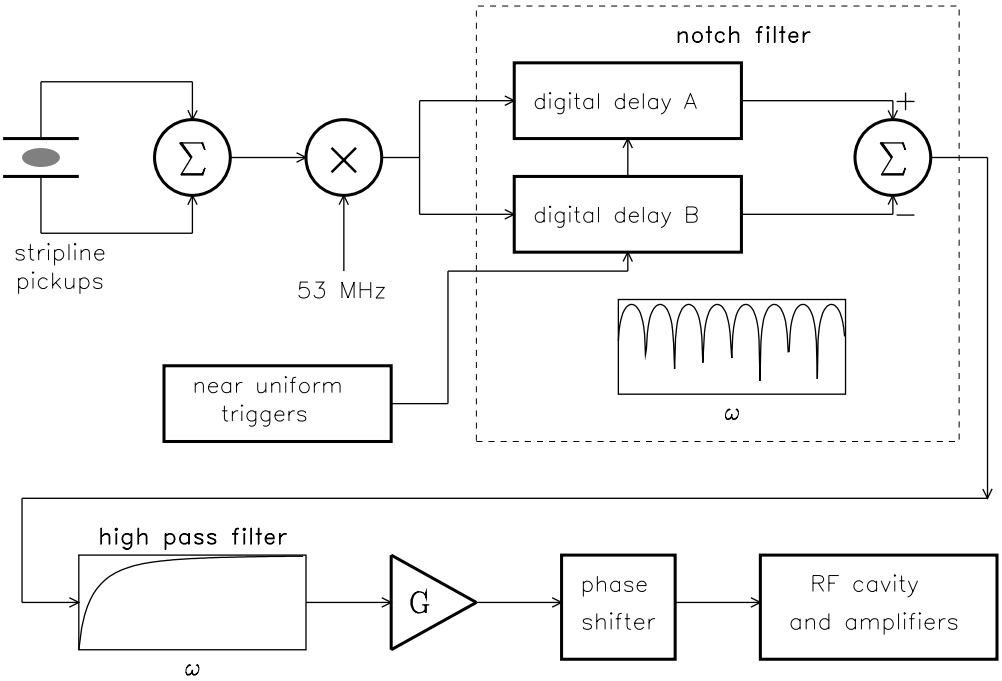

Figure 6. This figure shows the block diagram of the setup used for the longitudinal dampers.

3.1 Equalizer

The idea of using a hpf to equalize the impedance of the RF cavity comes from observing that if we model the RF cavity impedance Z_{RF} using an *RLC* circuit and define R_s is its shunt impedance, L is its inductance and C is its capacitance, then

$$Z_{\mathrm{RF}} = \frac{R_s}{1 - iQ\left(\frac{\omega_R}{\omega} - \frac{\omega}{\omega_R}\right)} \tag{3.1}$$

If $\omega_R = 1/\sqrt{LC}$ is its resonant frequency and $Q = R_s\sqrt{C/L}$ is its quality factor, then the magnitude $\left|Z_{\mathrm{RF}}\right|$ is

$$\begin{aligned} \left|Z_{\mathrm{RF}}\right| &= \frac{R_s}{\sqrt{1 + Q^2\left(\frac{\omega_R}{\omega} - \frac{\omega}{\omega_R}\right)^2}} \\ &= \frac{R_s}{Q\left|\frac{\omega_R}{\omega} - \frac{\omega}{\omega_R}\right|} \qquad \text{when } Q \to \infty \end{aligned} \tag{3.2}$$

If we write $\omega = \omega_R + \delta\omega$ so that $\delta\omega/\omega_R \ll 1$ (for example, in our system 47 kHz $< \delta\omega/2\pi <$ 1.25 MHz, $\omega_R/2\pi = 53$ MHz, and $Q \sim 10^4$), Eq. 3.2 becomes

$$\left|Z_{\mathrm{RF}}\right| = \frac{R_s}{2Q}\left|\frac{\omega_R}{\delta\omega}\right| \sim \left|\frac{\omega_R}{\delta\omega}\right| \tag{3.3}$$

which means that $\left|Z_{\mathrm{RF}}\right|$ has a $1/\delta\omega$ type dependence when $Q \to \infty$ and $\delta\omega/\omega_R \ll 1$.

Next, let us examine the response of a hpf. We introduce first a new variable $\Delta\omega = (\omega - \omega_{\mathrm{RF}})$ (the reason for doing this will become apparent later on in the analysis). ω_{RF} is the RF drive frequency and $\omega_{\mathrm{RF}} \approx \omega_R$. For a hpf with a 3 dB response at $\Delta\omega_{3\mathrm{dB}}$, its response function R_{hpf} is

$$R_{\mathrm{hpf}}(\Delta\omega) = \frac{1 + i\frac{\Delta\omega_{3\mathrm{dB}}}{\Delta\omega}}{1 + \frac{\Delta\omega_{3\mathrm{dB}}^2}{\Delta\omega^2}} \tag{3.4}$$

and when $\Delta\omega \ll \Delta\omega_{3\mathrm{dB}}$, we see that

$$\begin{aligned} R_{\mathrm{hpf}}\left(\Delta\omega \ll \Delta\omega_{3\mathrm{dB}}\right) &= i\frac{\Delta\omega}{\Delta\omega_{3\mathrm{dB}}} \\ \Rightarrow \qquad \left|R_{\mathrm{hpf}}\left(\Delta\omega \ll \Delta\omega_{3\mathrm{dB}}\right)\right| &= \left|\frac{\Delta\omega}{\Delta\omega_{3\mathrm{dB}}}\right| \end{aligned} \tag{3.5}$$

and thus $\left|R_{\mathrm{hpf}}\right|$ has a $\Delta\omega$ dependence. So now, we have to multiply the baseband response of the hpf by the impedance of the RF cavity which is strongest about ω_R to obtain a constant impedance.

3.2 Phase Shifter

A phase shifter is a device takes as input a voltage V_{in} and converts it to a phase shift $\Delta\phi$ in the RF. Suppose the conversion factor between voltage and angle is K rad/V and the RF to be shifted is $V_{\mathrm{RF}}\sin\omega_{\mathrm{RF}}t$ and $V_{\mathrm{in}}(\Delta\omega) = V_0 e^{i\Delta\omega t} R_{\mathrm{hpf}}(\Delta\omega)$, (See *Appendix I* of Reference [5]) , the output of the phase shifter is

$$V_{\Delta\phi}\,(\text{dipole mode}) = \frac{V_{\mathrm{RF}}}{2} K V_0 R_{\mathrm{hpf}}(\Delta\omega) e^{i\omega t} \tag{3.6}$$

from which we can just read off[2] the dipole mode response of the hpf phase shifter combination as

$$\left|R_{\mathrm{hpf}+\Delta\phi}(\omega)\right| = \left|\frac{V_{\mathrm{RF}}}{2} K R_{\mathrm{hpf}}(\Delta\omega)\right| \sim \left|\frac{\Delta\omega}{\Delta\omega_{3\mathrm{dB}}}\right| \tag{3.7}$$

Therefore, $R_{\mathrm{hpf}+\Delta\phi}(\omega) Z_{\mathrm{RF}}(\omega)$ will have a constant impedance in the region around $\omega_R \approx \omega_{\mathrm{RF}}$ and $\left|\omega_{\mathrm{RF}} - \omega\right| \ll \omega_{3\mathrm{dB}}$ as required. In the design, we chose $f_{3\mathrm{dB}} = 2$ MHz

[2]There is a subtlety here, since the phase shifter is a non linear device which means technically there the frequency response is undefined. However, by introducing $\Delta\omega$ which is equivalent to a down converted signal, we can talk of a response.

3.3 Notch Filter

The notch filter used in the electronics serves a two fold purpose. First, it suppresses the revolution harmonics. Second, it differentiates the synchrotron sidebands around the revolution harmonics which tells the damper which direction to kick. In our setup, the notch filter is created with two digital delay lines. Its response is given by

$$R_{\text{notch}}(\omega) = 1 - e^{-i\omega NT} \tag{3.8}$$

where T is the revolution period and N is the number of revolution periods in the delay. We will see later in this section that the choice of N is a compromise between the synchrotron frequency of the Tevatron at 150 GeV and 980 GeV.

The notch filter clearly suppresses the revolution harmonics at $\omega_0 = 2\pi f_0$ since $R_{\text{notch}} = 0$ whenever

$$\begin{aligned} \omega &= 2M\pi/NT \qquad M \in \mathbb{Z} \\ f &= \frac{M}{N} f_0 \end{aligned} \tag{3.9}$$

i.e. a notch appears at every multiple of the revolution harmonic f_0 whenever M is a multiple of N. Another observation is that the number of notches between 0 and f_0 is N.

The block diagram of the actual implementation of the digital notch filter is shown in Figure 7. A full discussion on how the notch filter is built is in ref. [6]. The filter consists of one 14-bit digitizer, two 64k-value asynchronous FIFO memories, a 14-bit ALU, one 14-bit DAC, and two counters. The input signal is digitized and loaded into both FIFOs. The FIFOs hold the data for the number of clock ticks specified by the counters and then out put their data to the ALU. The ALU performs the desired math function on the data and drives the input to the DAC. The output signal comes from the DAC.

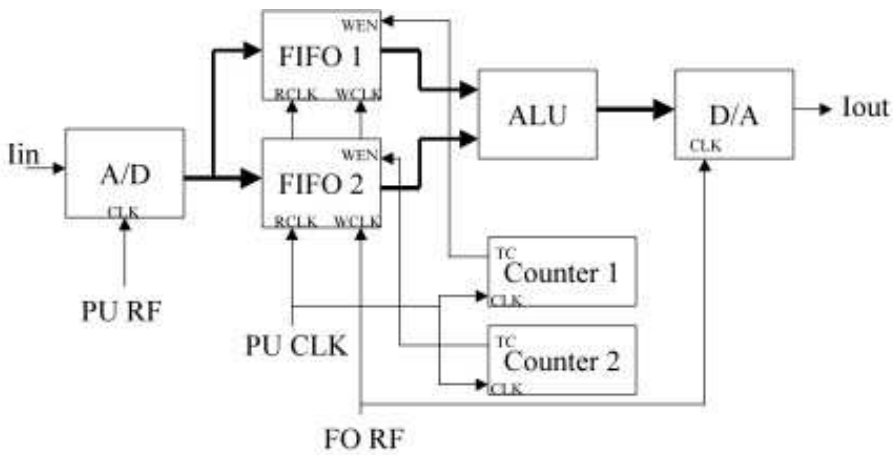

Figure 7. Block diagram of the digital notch filter card.

3.3.1 Differentiator

To show that the slope of the notch around the synchrotron frequency is a differentiator, let us choose an $M = 1$ notch at $2\pi/NT \equiv \omega_z$ (Obviously, any $2M\pi/NT$ will work). The synchrotron

frequency near this notch is $\Omega_s = \omega_z + \omega_s$, which means that the response of the notch filter at Ω_s is

$$\begin{aligned} R_{\text{notch}}(\Omega_s) &= 1 - e^{-i\Omega_s NT} = 1 - e^{-i\omega_s NT} \\ &= 2\sin\frac{\omega_s NT}{2} e^{i\varphi} \end{aligned} \tag{3.10}$$

where $\tan\varphi = \sin\omega_s NT/(1-\cos\omega_s NT)$. Now when $\omega_z \neq 0$, we have $\omega_s NT = 2\pi\omega_s/\omega_z \approx 0$ if $\omega_s \ll \omega_z$, so that $\varphi = \pi/2$, then

$$R_{\text{notch}}(\Omega_s) \approx i\omega_s NT + \ldots = i(\Omega_s - \omega_z)NT + \ldots \tag{3.11}$$

which to first order in $\omega_s NT$ has differentiated in time the synchrotron sidebands at Ω_s.

As we have mentioned earlier, the choice of N are compromises between the Tevatron's injection energy at 150 GeV and its top energy at 980 GeV and the phase and amplitude responses at these two energies. We chose $NT = 1/6f_s$ where $f_s \approx 88$ Hz is the synchrotron frequency at 150 GeV. Therefore, $N = 90$ when $T = 21$ µs. (Note: we have actually set $N = 91$ in the real setup).

3.4 Near Uniform Triggers

In order for the digital delays to work they have to be triggered. The triggers which we use are nearly uniform in time. The reason for the non-uniformity in triggers comes from the spacing of the bunches in the Tevatron. At present, there are three trains of 12 bunches. In each train, the bunches are spaced 21 buckets apart. The spacing between the trains are the abort gaps and they take up 140 buckets each. As a check, we can add these numbers up $3 \times (21 \times (12-1) + 140) = 1113$ which is exactly the harmonic number of the Tevatron. Notice that 21 does not divide the number of buckets in the abort gap. This observation threw us off initially when we had triggers which were uniformly spaced 21 buckets apart. We fixed this by having triggers at the following bucket locations:

in train	in abort gap
$\mathbf{1}, \mathbf{22}, \mathbf{43}, \ldots, \mathbf{211}, \mathbf{232}$	$253, 274, \ldots, 337, 358$
$\mathbf{372}, \mathbf{393}, \mathbf{414}, \ldots, \mathbf{582}, \mathbf{603}$	$624, 645, \ldots, 708, 729$
$\mathbf{743}, \mathbf{764}, \mathbf{785}, \ldots, \mathbf{582}, \mathbf{603}$	$624, 645, \ldots, 1079, 1100$

which has mostly a 21 bucket spacing with the exceptions being between the last bucket of the abort gap and the first bucket of the train when we only have 14 buckets.

The reason for having near uniform triggers rather than having triggers where the bunches are is to allow us to use reasonable cable delays to ensure that the correct bunches are kicked. In the worst case scenario for near uniform triggers, the cable length will be 21 buckets$/2 \approx 200$ ns for correctly hitting the right bunch. While for triggers where there are bunches only, the worst case scenario will be 140 buckets$/2 \approx 1.3$ µs of cable!

3.5 Phase Shifts

There are three devices in the damper circuit which introduce phase shifts. They are:

(i) RF cavity, around the resonance $\delta\omega \ll \omega_R$.

(ii) High pass filter, at base band $\omega \ll \omega_{\mathrm{RF}}$.

(iii) Notch filter, at every revolution harmonic ω_0.

Shown in Figure 8 are the magnitudes and phase shift response of each of the devices. For each of the devices we can make the following approximations:

(a) RF cavity: shifts the phase $\pi/2$ below resonance and $-\pi/2$ above resonance.

(b) High pass filter: the phase shift is $+\pi/2$ phase shift when $0 < \omega \ll \omega_{3\mathrm{dB}}$.

(c) Notch filter: near the notch, the phase shift is $-\pi/2$ below the notch and $+\pi/2$ above the notch.

As an example, let us use the response of the synchrotron sidebands at $\omega_{\mathrm{RF}} + \omega_0 \pm \omega_s$ and pass them through the RF cavity. Now the RF cavity rotates the imaginary part according to (a) and thus the real part of the result is anti-symmetric about ω_R. When we down convert this signal, we should measure sidebands about ω_0 which have anti-symmetric real parts. See Figure 9(b). The process is actually a bit complicated because mixers are non-linear devices. In order to have zero phase shift from down-conversion, we have to assume that the up and down-conversion occur in pairs, i.e. the synchrotron sidebands are measured from a down-converted signal which is excited with an up-converted signal. The resultant phase when the signal is down-converted and then up-converted is zero.

Next, when the down-converted signal goes through the high pass filter, both sidebands are rotated by $+\pi/2$, and thus the imaginary part must now be antisymmetric. See Figure 9(c).

Finally, when we take this signal and pass it through a notch filter, they become perfectly symmetric! And if we have the sign of the gain right, they will be symmetric and negative which is exactly what is required for damping. See Eq. 2.9 and Figure 9(d).

3.6 Problem with Mode 0

The dampers do not work on mode 0. If we go through the rotations in phase from each element as we did in section 3.5, we will find that the real part of the response is anti-symmetric about $\omega = 0$. The source of the problem is that the high pass filter has a phase shift of $-\pi/2$ when $-\omega_{3\mathrm{dB}} \ll \omega < 0$. However, we notice that the gain near ω_0 is small because of the hpf and the notch filter and thus mode 0 will not be anti-damped. Mode 0 must be taken care of by the Robinson stability criterion by tuning the cavities so that its fundamental resonance is lower in frequency than the RF frequency.

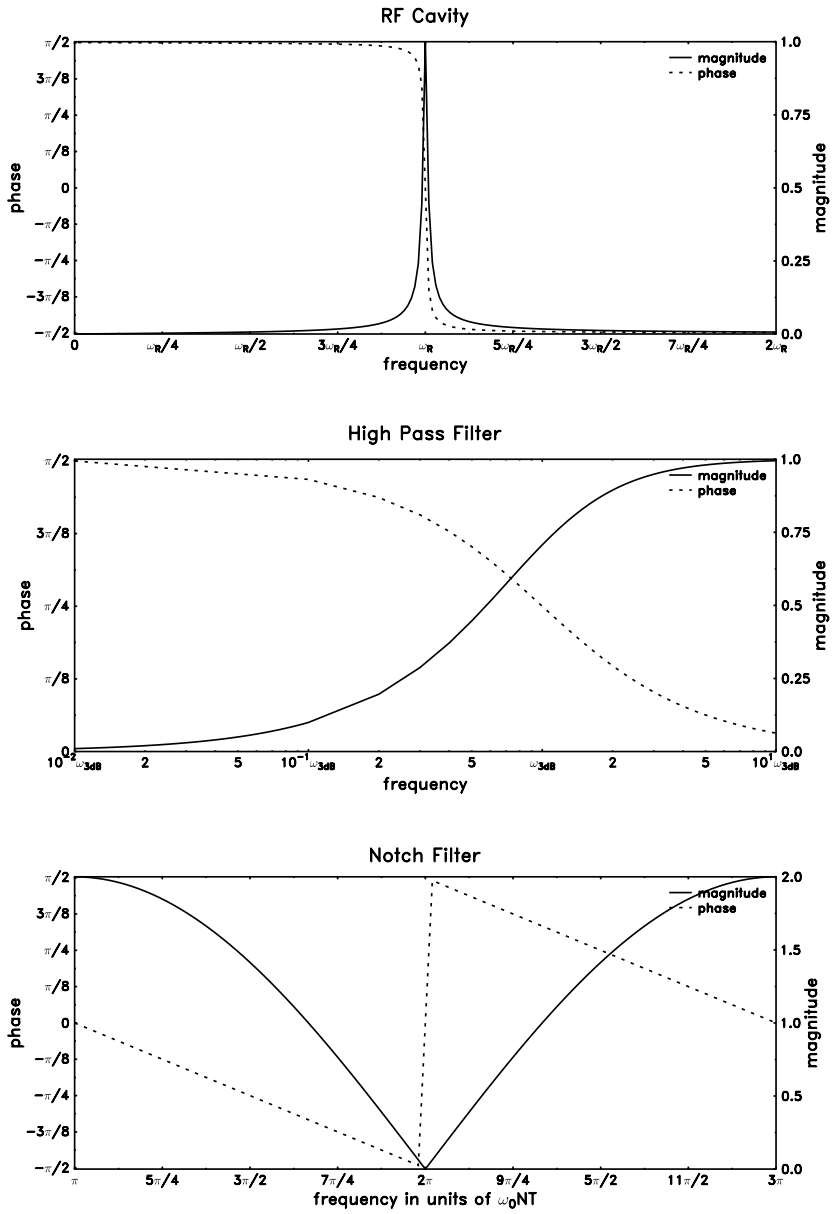

Figure 8. The magnitude and phase responses of three of the devices in the damper circuit.

3.7 Setting up the 1 turn delay

We set up the 1 turn delay by performing the measurement with delay B disconnected. See Figure 10. When this is done, we can get the response to look like Figure 9(c). Three of the possible

26 modes are shown in Figure 11. Before the correct amount of delay is set in Delay A, the as found imaginary part of the response is the top graph in Figure 11. When the delay is made exactly right, we get the anti-symmetric imaginary responses for all the modes. Three of the modes are shown as examples in the bottom graph of Figure 11.

3.8 Making the notches

After the delay has been set in Delay A, we can make the notches by reconnecting back Delay B and by setting the delay in this card by $N(=91)$ revolution periods w.r.t. Delay A. (The value of N was calculated in the subsection 3.3). The notches do not land perfectly on each revolution harmonic because the electronics in each card are not exactly the same and so there is some small error in delay. This can be fixed by adding a a length of cable between Delay A and Delay B by using the method discussed in *Appendix III of ref. [5].* This method works really well and we find that the notches will land exactly on the revolution harmonics. However, the two cards do not have exactly the same gain and serendipitously, a shorter cable (and thus a smaller attenuation) actually gives a better notch, albeit not exactly on the revolution harmonic. The results are shown in Figure 12.

Finally, after the notch filter has been added into the circuit into the circuit the frequency response can be measured using the same block diagram shown in Figure 10 but with delay B reconnected. Like we had previously discussed and shown in Figure 9(d) with the gain set to -1, the real part of the response is negative and symmetric. These results are shown in Figure 13. The top graph of Figure 13 shows the response at 150 GeV and the bottom graph is at 980 GeV.

3.9 Limits on the gain

The main limitation on the gain of the dampers are the "wings" indicated in Figure 13. As we increase the gain, the wings become more positive and when it gets comparable in size to the negative real part, the damper anti-damps the beam.

We measured the open loop transfer measurements up to the twentieth revolution harmonic (See Figure 13) and we can see that the amplitude of the wings get progressively worse as the mode number increases. However, for the gain setting of -5 used for high energy physics (HEP), the wings do not present a problem. This setting is about 20% below the gain margin of the system.

3.10 Tests

To test whether the dampers indeed work, we excite the beam at 980 GeV by switching the sign of the gain. This is a good sign because we can actually excite the beam which means that there is sufficient gain in the loop. When we switch the sign of the gain back to damping, we find that the excitation can be damped. The results of these actions are shown in Figure 14. Although the dampers do perform their job, we find that damping takes 2 to 3 minutes in these examples.

4. Damper Performance during Stores

The initial luminosity recorded at the experiments has increased by a factor of 400 from about (1×10^{30}) cm^{-2}s^{-1} of store 460 in 2001 to the record initial luminosity of (424×10^{30}) cm^{-2}s^{-1} of store 8709 in 2011. The luminosity increase can be seen Figure 15. Most of the luminosity increase can be accounted from the larger number and smaller emittance of anti-protons at collisions.

The proton longitudinal instability has been well controlled by the dampers. But there are mysteries as to why instabilities are observed hours into a store where the bunch length is longer and the proton intensity is lower than at the start of HEP. See Figure 16. The bunch length growth after each incident is $\sim$0.5% which does not affect the experiments.

5. Conclusion

The dampers have worked very well in controlling the instabilities in the Tevatron. For the past 9 years, the electronics have proved to be extremely reliable and we have done very little maintenance work on them. However, the source of these instabilities have not be identified and there is a bigger mystery as to why the beam becomes unstable well into a store. We have not made or considered any improvements of the damper system because the damper system has met all the operational requirements for high energy physics

A. Some Parameters of the Tevatron

Table 2. Comparison of different stores

Symbol	Description	Value
h	harmonic number	1113
–	number of proton bunches	36
–	number of buckets between bunches in a train	21
–	number of buckets between trains	140
–	bucket size	18.8 ns
f_0	revolution frequency at 150 GeV	47.712 kHz
f_{RF}	frequency of RF drive at 150 GeV	53.103639 MHz
f_s	synchrotron frequency at 150 GeV	88 Hz
f_0	revolution frequency at 980 GeV	47.713 kHz
f_{RF}	frequency of RF drive at 980 GeV	53.104705 MHz
f_s	synchrotron frequency at 980 GeV	34 Hz

Acknowledgments

This work is supported by Fermi Research Alliance, LLC under Contract No. DE-AC02-07CH11359 with the United States Department of Energy.

References

[1] S. Pordes *et al*, *Signal Processing For Longitudinal Parameters Of The Tevatron Beam*, in proceedings of *Particle Accelerator Conference* May, 12 – 16, 2005 Knoxville, TN.

[2] F. Pedersen, *RF Cavity Feedback*, *CERN document* (1992), CH-12- 1211.

[3] J. Dey and I. Kourbanis, *53 MHz Beam Loading Compensation for Slip Stacking in the Fermilab Main Injector* in proceedings of *Particle Accelerator Conference* May, 12 – 16, 2006 Knoxville, TN.

[4] D. McGinnis, *Introduction to RF Systems*, *U.S. Particle Accelerator School* held at Duke University, 1995.

[5] C.Y. Tan and J. Steimel, *The Tevatron Bunch by Bunch Longitudinal Dampers*, *Fermilab Technical Memo* (2002) TM-2184.

[6] J. Steimel, *Digital Notch Filter Operating Manual*, *Beams Document* (2002) Beams-doc-204-v1.

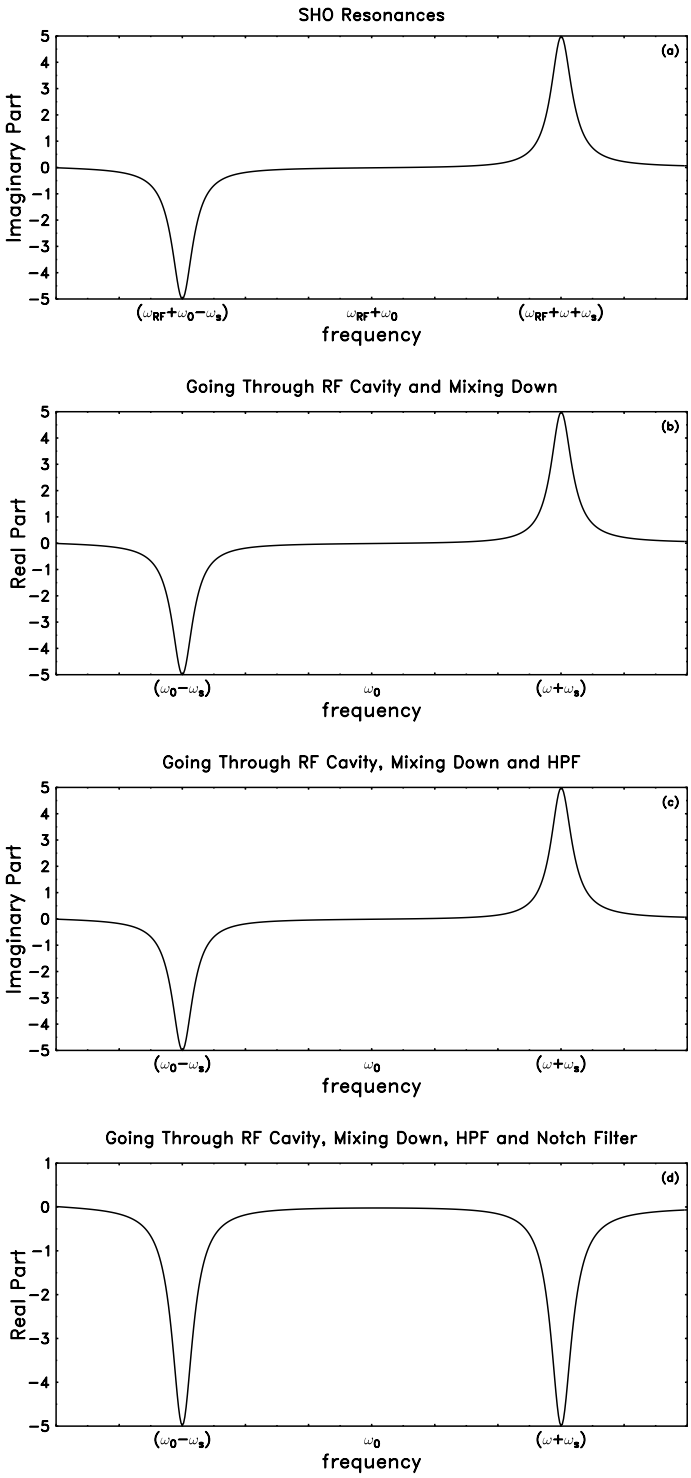

Figure 9. These figures show the upper and lower synchrotron sidebands (a) modeled as the response of a simple harmonic oscillator (sho). The response after going through each device which contributes a phase shift are plotted here.

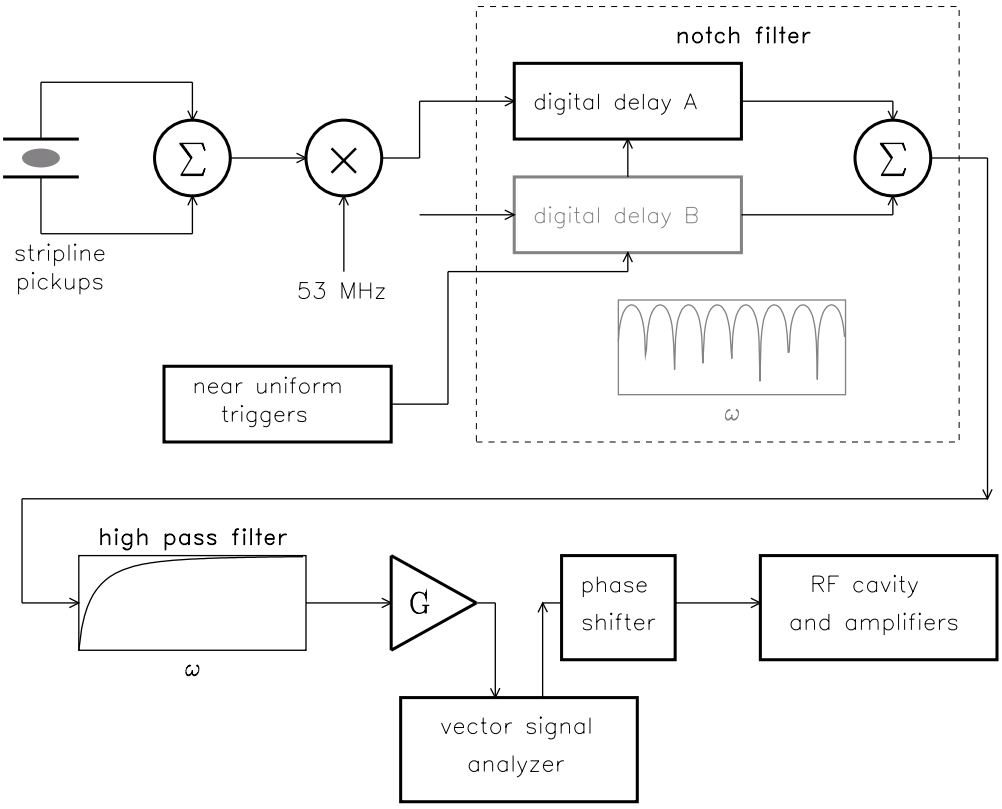

Figure 10. To get the 1 turn delay correct, we disconnected digital delay B and measured the response. For the open loop measurement discussed in section 3.8 we connect delay B back into the circuit.

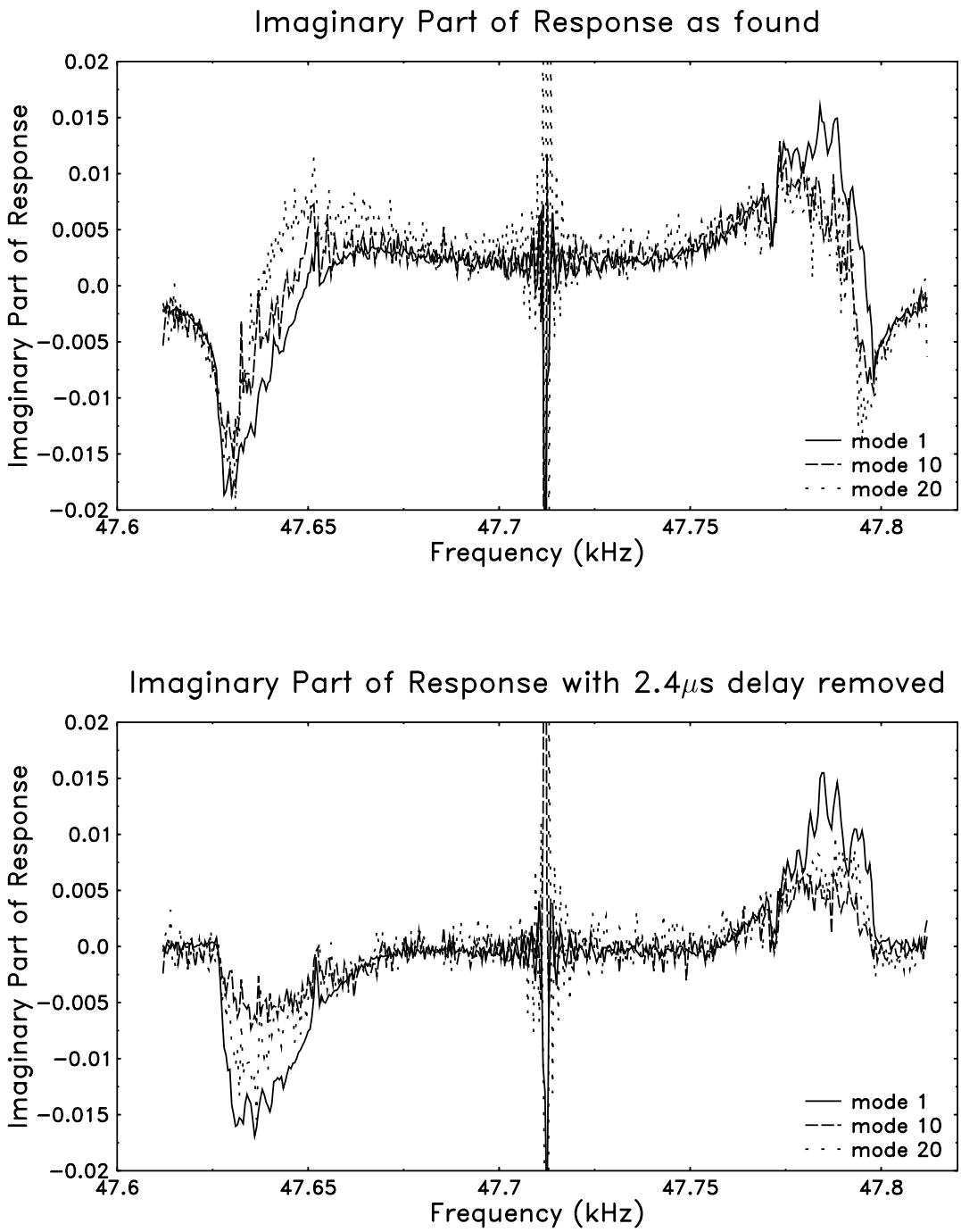

Figure 11. These graphs show the imaginary part of the response of modes 1, 10 and 20 before and after the delay was corrected. We have superimposed all the three graphs on top of each other by shifting the frequency of mode 10 by $-10f_0$ and mode 20 by $-20f_0$.

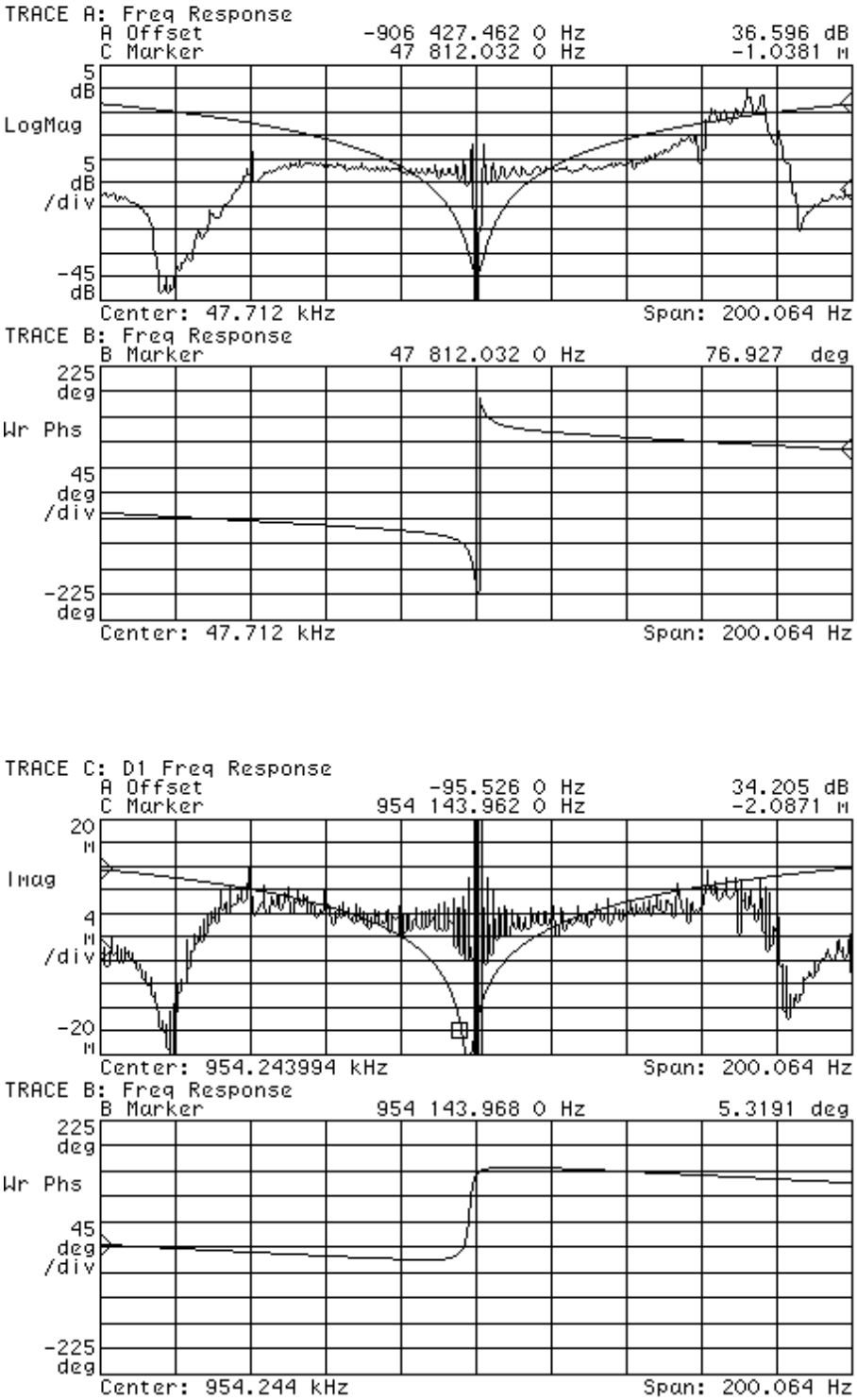

Figure 12. With both delays in the loop, we get notches near the revolution harmonics. The uncorrected imaginary response with one digital delay is superimposed for reference. See text for more details

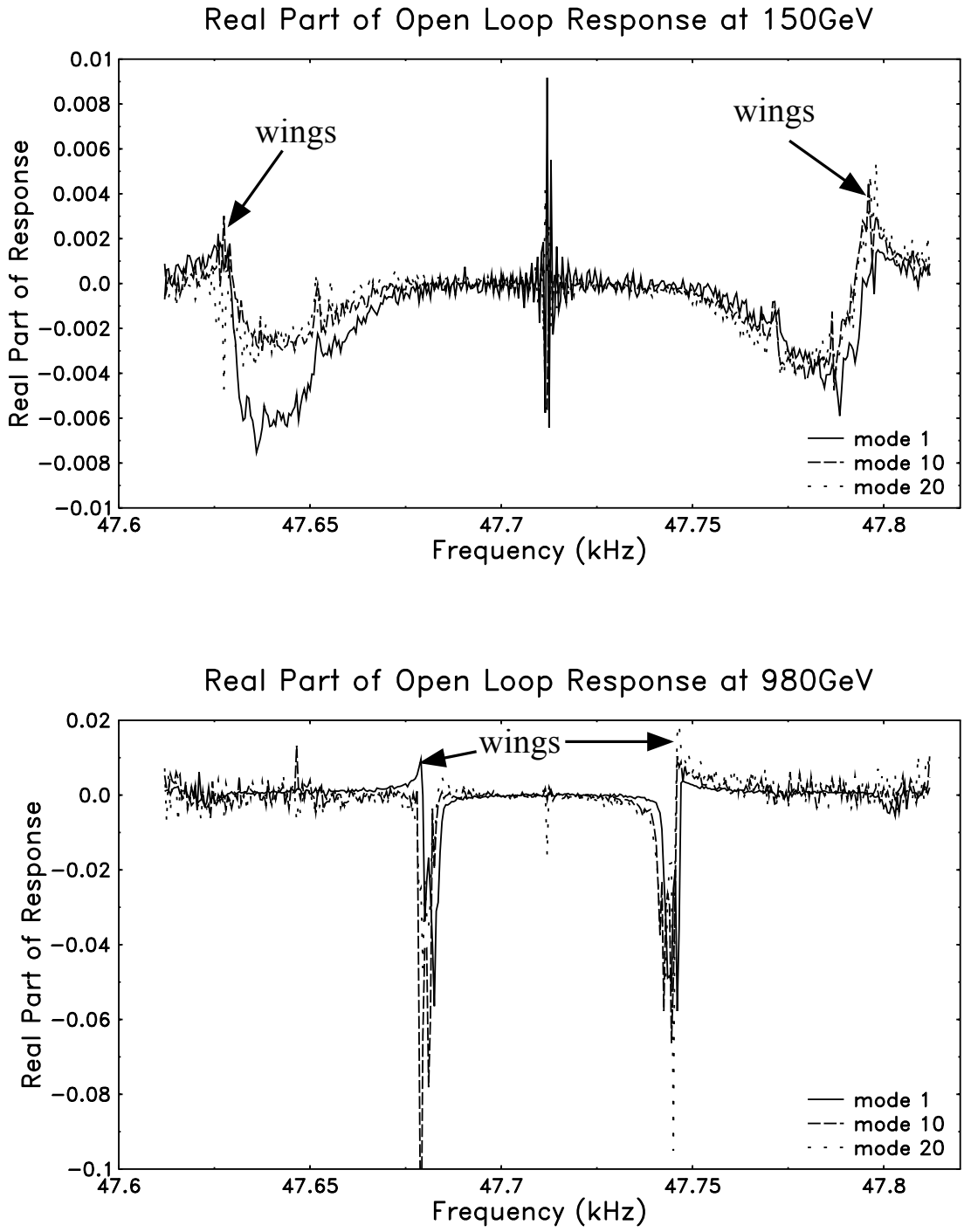

Figure 13. These graphs show the real part of the open loop response of modes 1, 10 and 20 at 150 GeV and 980 GeV. We have superimposed all the three graphs on top of each other by shifting the frequency of mode 10 by $-10f_0$ and mode 20 by $-20f_0$. The limitations on the gain of the system are the "wings".

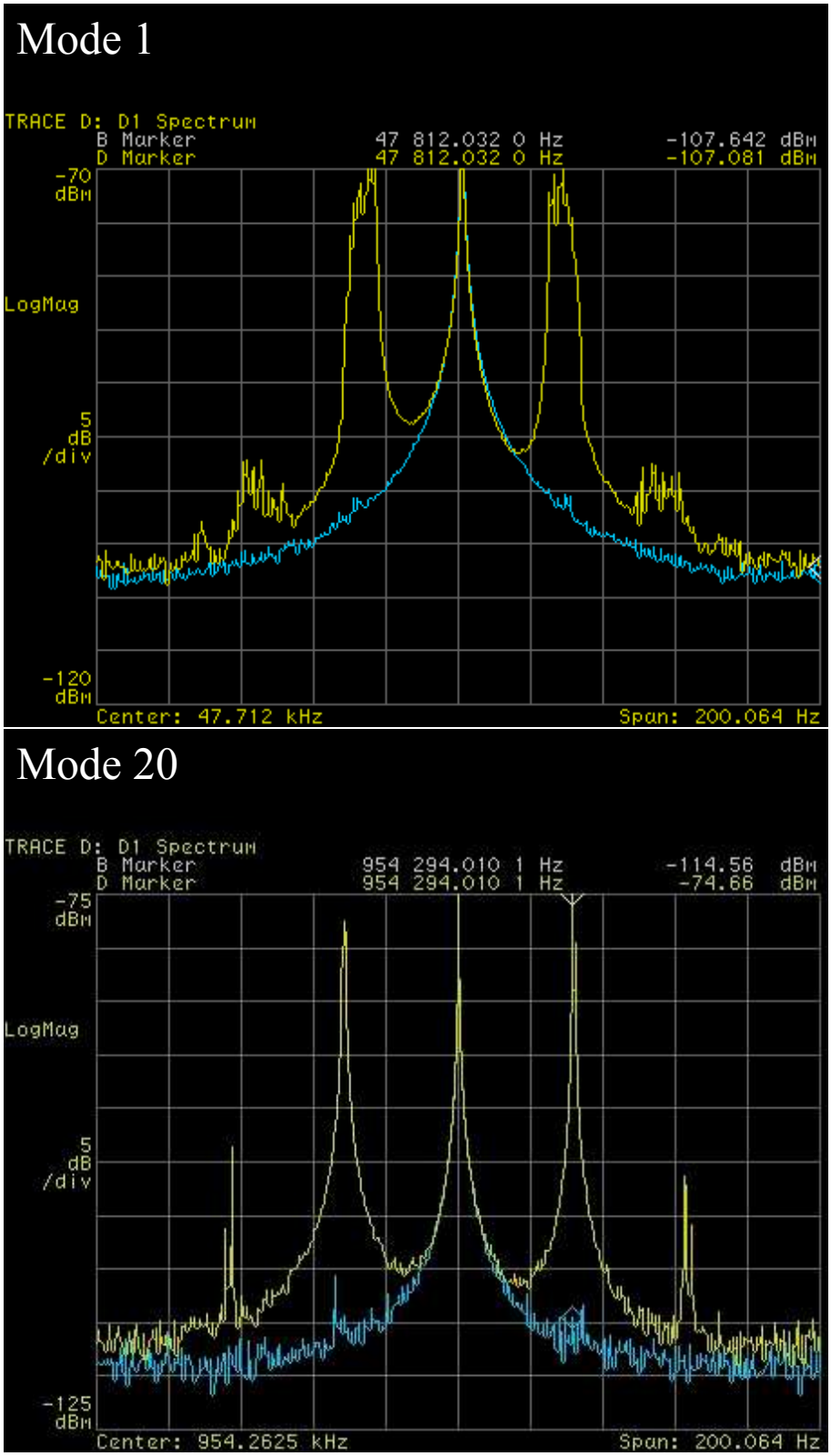

Figure 14. When we closed the loop at 980GeV, we excited the beam by anti-damping it. Then we turned on damping and clearly the synchrotron lines of mode 1 and 20 were damped.

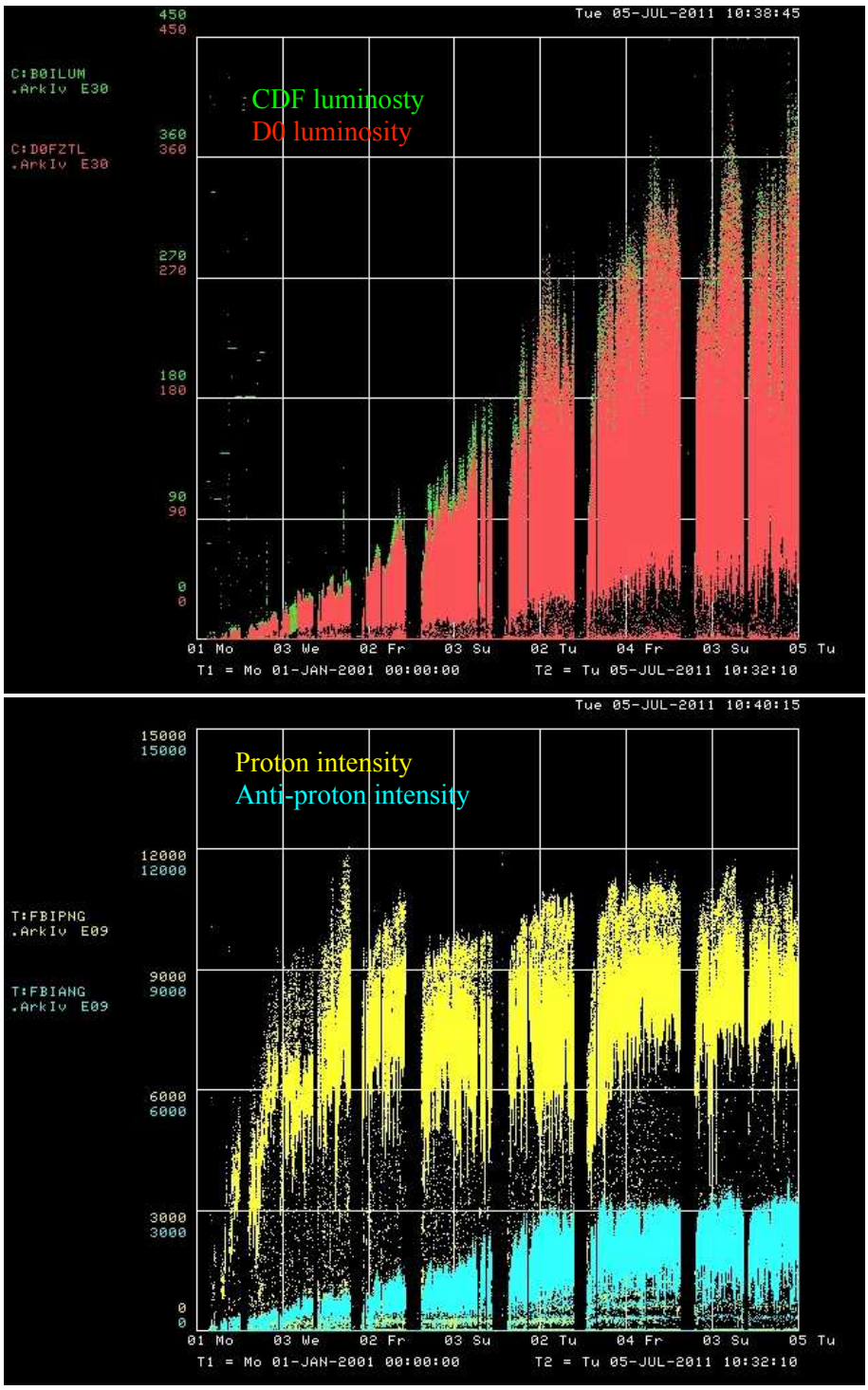

Figure 15. The luminosity at the experiments CDF (green points) and D0 (red points) has increased by a factor of 400 from 2001 to 2011. The peak proton intensity (yellow points) during this time is about 12000×10^9 protons in 2003. The corresponding increase in luminosity mainly comes from both decrease in emittance and the increase in anti-proton intensity (cyan points) from about 400×10^9 in 2002 to 3000×10^9 in 2011..

Figure 16. In store 7477, the proton longitudinal bunch length (T:SBDPWS) made two attempts to blow up 1 hour into HEP but the dampers were able to stop them. The bunch length increase is very small during these two instabilities $\sim$0.5%. The proton intensity (T:SBDPIS) has already decreased by about 1.5% and the bunch length has already increased by about 6% just before the onset of instability.